ARL-TR-7776 ● SEP 2016

US Army Research Laboratory

Tritiation and Stability Measurements of Nitroxide for Betavoltaic Cells

by J Russo, G Rosen, D Bigio, M Litz, and W Ray II

NOTICES

Disclaimers

The findings in this report are not to be construed as an official Department of the Army position unless so designated by other authorized documents.

Citation of manufacturer's or trade names does not constitute an official endorsement or approval of the use thereof.

Destroy this report when it is no longer needed. Do not return it to the originator.

ARL-TR-7776 ● SEP 2016

US Army Research Laboratory

Tritiation and Stability Measurements of Nitroxide for Betavoltaic Cells

by J Russo, M Litz, and W Ray II
Sensors and Electron Devices Directorate, ARL

G Rosen and D Bigio
University of Maryland, College Park, MD, and
Organic Electronic Devices, LLC

REPORT DOCUMENTATION PAGE

Form Approved
OMB No. 0704-0188

1. REPORT DATE *(DD-MM-YYYY)*	2. REPORT TYPE	3. DATES COVERED (From - To)
September 2016	Technical Report	1 February–1 May 2016

4. TITLE AND SUBTITLE
Tritiation and Stability Measurements of Nitroxide for Betavoltaic Cells

5a. CONTRACT NUMBER

5b. GRANT NUMBER

5c. PROGRAM ELEMENT NUMBER

6. AUTHOR(S)
by J Russo, G Rosen, D Bigio, M Litz, and W Ray II

5d. PROJECT NUMBER

5e. TASK NUMBER

5f. WORK UNIT NUMBER

7. PERFORMING ORGANIZATION NAME(S) AND ADDRESS(ES)
US Army Research Laboratory
ATTN: RDRL-SED-E
2800 Powder Mill Road
Adelphi, MD 20783-1138

8. PERFORMING ORGANIZATION REPORT NUMBER
ARL-TR-7776

9. SPONSORING/MONITORING AGENCY NAME(S) AND ADDRESS(ES)

10. SPONSOR/MONITOR'S ACRONYM(S)

11. SPONSOR/MONITOR'S REPORT NUMBER(S)

12. DISTRIBUTION/AVAILABILITY STATEMENT
Approved for public release; distribution unlimited.

13. SUPPLEMENTARY NOTES

14. ABSTRACT
Beta radioisotope energy sources, such as tritium (^{3}H), have shown significant potential in satisfying the needs of an energy-driven world. The drawbacks of current beta source compounds include low beta-flux power, intrinsic isotope leakage, and beta self-absorption. The figure of merit for a tritiated compound is the input power or specific surface activity of the thin layer (Ci/cm^2) where an optimal portion of incident beta particles are penetrating the semiconductor depletion region. The goal is to synthesize a compound with an effective surface activity (from one side) of 30 mCi/cm^2 where it can be used for both planar and high aspect ratio, textured structures (pillared, etched, etc.). Nitroxides are chosen to meet these requirements because of physical properties (solid and pliable at standard temperature and pressure and controllable deuteration and hydrogenation synthesis from previous published work). Calculations show that only 1 of the 4 compounds can possibly meet short-term goal of approximately 30 mCi/cm^2, but its tritiation stability during and after synthesis is unknown. As a proof of concept with respect to tritiation, the nitroxide 4-methoxycarbonyl-methylene-2,2,6,6-tetramethyl-1-piperidinyloxyl (TEMPO) is tritiated (^{3}H) with a specific activity of 103 Ci/g. The stability of TEMPO containing tritium in a solution of toluene is achieved. TEMPO in toluene is found to be 100% stable at least up to 27 days, when the experiments are terminated, as no loss of tritium from a solution of this nitroxide is observed.

15. SUBJECT TERMS
tritium organic compound, betavoltaic cell, nitroxide, gallium nitroxide, long-term energy storage

16. SECURITY CLASSIFICATION OF:			17. LIMITATION OF ABSTRACT	18. NUMBER OF PAGES	19a. NAME OF RESPONSIBLE PERSON
a. REPORT	b. ABSTRACT	c. THIS PAGE			19b. TELEPHONE NUMBER (Include area code)
Unclassified	Unclassified	Unclassified	UU	50	Johnny A Russo 301-394-5530

Standard Form 298 (Rev. 8/98)
Prescribed by ANSI Std. Z39.18

Contents

List of Figures

List of Tables

1. Introduction

The 2 main categories of isotope energy sources are betavoltaic and beta-photovoltaic cells. Betavoltaic cells are direct conversion systems, converting beta radiation energy into usable electrical energy through semiconductor energy conversion devices. In general, they are typically more efficient ranging from 1% to 20% depending on the beta radioisotope source.[1–3] Betaphotovoltaic cells are indirect energy systems, converting beta radiation energy to radioluminescence photon emission via a scintillating material, either powder or single crystal form, to usable electrical energy through direct bandgap semiconductor energy conversion devices. So far, the overall energy conversion efficiency ranges from 0.1%–2% depending on the beta radioisotope source.[4–6] The similarities between both systems are the beta source form and electron-hole pairs (EHPs) generation in the semiconductor. One main purpose of radioisotope sources is powering environmental monitoring sensors for longer than a decade. The mission requires minimal source volume and footprint, and no need for battery replacement to lower the costs and dangers to personnel. The power output range is normally between 0.1 to 100 μW_e.[6]

The most practical beta sources are nickel-63 (^{63}Ni) and tritium (^{3}H), which have a half-life of 100 and 12.3 years and average beta energy of 17.4 and 5.7 keV, respectively. Low-energy beta particles provide enhanced lifetimes due to the absence of semiconductor degradation. Tritium is the isotope of choice because it has low toxicity, beta energy less than 20 keV, and it is the least expensive per kilogram and kilojoule of all beta-emitting radioisotopes. Tritium has a comparable energy density and greater power density than ^{63}Ni. Finally, the higher beta energy spectrum of ^{63}Ni causes the betavoltaic cell to be less efficient with current structures. A median layer would need to be implemented to slow down high-energy betas from passing through the depletion region in the semiconductor.

Tritium is the most viable beta source to construct the most efficient betavoltaic cell. Nevertheless, it has setbacks and constraints with respect to physical form of a gas at standard temperature and pressure (STP). Tritium has to be contained physically in a vessel or chemically bonded in a compound. Gaseous tritium at STP has the highest specific activity (A_m) at 9,650 Ci/g and specific beta flux power (dP_β/dS) of 8.73 $\mu W_n/cm^2$ (Table 1).[7] The values are considered the maximum limit for tritium.

Table 1 Theoretical calculations of tritiated compounds. Some of the values are averages due to tritiation yield fluctuations. Li^3H has the highest S_m but is pyrolytic, eliminating it from comparison to other compounds. Graphane-like nanofibers show potential but still are far from even controlling hydrogenation yield consistency in microscale-systems. Metal hydrides are widely used in current technologies but are limited by beta range depth and planar beta emission. Appendix A explains the formulation of these parameters.

Tritiated compound type	Specific activity (A_m) (Ci/g)	Mass density (ρ_m) (g/cm^3)	Gravimetric density (GD) (wt% ^{3}H)	Volume activity (V_m) (Ci/cm^3)	FOM_{2D} specific beta flux power at $D_{0.99}$ ($\frac{dP_\beta}{dS}$); $\left[\frac{\mu W_n}{cm^2}\right]$	Beta range depth ($D_{0.99}$) (µm)	FOM_{2D} Effective surface activity (S_m) (mCi/cm^2)
TiT_2 = Ti^3H_2	1100[a,b]	3.91[a,b]	4–12.5[a,b]	4300[a]	Exp. 0.73[c] Max. 0.99[a]	D_L = 0.4[c,d] $D_{0.99}$ = 0.77[a,b]	Max. (30)[a] Exp. (15)[c]
LiT = Li^3H	2910[a,b]	0.816[a,b]	25–30[a,b]	2317[a,b]	Max. 2.6[a,b]	3.7[a,b]	Max. (77)[a]
Tritiated organic compounds/ polymers	100–1000[a]	1.0[a]	1–10[a]	100–1000[a]	0.09–0.9[a]	3.0[a]	Max. (27)[a]
Graphane-like nanofibers [$(CH)_n$ only]	1649–2425[a]	Micro. system 0.28± 0.08[e,f]	Nanoscale-system (25%) Microscale-system (15–17%) [e,f]	461–679	Max. 2.2	4.7[g]	Max. (65)

Notes:
[a] Bower et al.[7]
[b] Belovodskii et al.[15]
[c] Thomas et al.[1]
[d] Layer thickness (D_L) for betavoltaic cell following Thomas et al.[1] approach.
[e] Nechaev[16]
[f] Sofo et al.[17]
[g] ESTAR calculations at average ^{3}H beta energy of 5.7 keV.[18]

The US Army Research Laboratory (ARL) was able to purchase commercial-off-the-shelf (COTS) ^{3}H gas-filled glass vials with a dP_β/dS of 4.1 $\mu W_n/cm^2$ with an effective surface activity (S_m) of 100 mCi/cm^2.[6] The gas has to be kept in a hermetic case at a certain pressure, which prohibits the device from being compact. The tritium gas has the lowest volume activity (V_m) of 2.60 Ci/cm^3 and power density of 87 W_n/cm^3 compared to other tritiated metal hydrides unless the pressure increases while temperature decreases.[8] These additional requirements make it difficult to fabricate and sustain power source function in the field, especially for a space-constrained application.

Metal hydrides have demonstrated higher V_m and power density, reaching closer to ^{3}H gas A_m, dP_β/dS, and S_m. Non-pyrolytic metal hydrides such as titanium tritide ($Ti^3H_{1.6}$) and scandium tritide (Sc^3H) have effective surface activities of 20 and 15 mCi/cm^2, respectively.[1,8] The results for dP_β/dS $Ti^3H_{1.6}$ and Sc^3H were 0.7 and 0.5 $\mu W_n/cm^2$. Table 1 lists additional tritiated compound metrics. The loading processes of tritium in these materials require extreme temperatures. The main

challenge in making the thin-film/substrate interface occurs during the loading process. Tensile and compressive stresses develop at the thin-film/substrate interface due to conflicting thermal expansion coefficients, where these stresses cause the thin-film layers to delaminate and buckle from the semiconductor surface. The main disadvantage of thin films is the thickness limit due to beta self-absorption or self-shielding where charged particles scatter through the material and slow down. Thicknesses of less than 500 nm are necessary for optimal efficiency of betavoltaic cells.[9] Tritiated metal hydrides are limited to a single side of beta emission collection because of the palladium layer used for the tritiation process. Tritium gas dissociation is similar to hydrogen dissociation for fuel cell applications. The palladium layer blocks a significant percentage of beta emission on the other side of the metal foil. Thomas et al. states that their metal hydride thickness is 400 nm before input beta flux power saturation due to self-absorption in the thin layer.[1] The 2-D geometric constraint limits the beta particle flux entering the depletion region of the semiconductor for EHPs generation and collection.

Polymers have been selected as candidates for beta sources and radioluminescent light sources. Several polymer chemical forms have been tested such as polystyrene, polyethylene (PE), polycarbonates (PC), polyurethanes, polyamides, and simple hydrocarbons like benzene.[10] Most tritiated polymers are synthesized using catalytic hydrogenation. There are fluctuating specific activity results ranging from 50 to 600 Ci/g depending on the synthesis procedure and structure of labeled polymer.[10] The advantages of tritiated polymers are that they are deformable and easier to manipulate for system fabrication, 3-D fabrication, low beta self-absorption, organic compounds, and low cost. The disadvantages are low gravimetric density (*GD*, wt% ^{3}H), low specific activity (A_m), and low production yield.

Carbon forms are other organic compound carrier candidates that show great promise in storing comparable tritium/hydrogen concentrations of metal hydrides, but they are more stable, have higher binding energies, and have less beta self-absorption due to lower density. They can store hydrogen through chemisorption (chemical bond) and physisorption (van der Waals [vdW] bonding). Carbon nanotubes (CNTs) have an experimental *GD* of 5 to 10 wt% hydrogen. They are chemically stable and have a low mass density.[10] The capillary effect of CNTs shows high concentration of hydrogen/tritium through vdW bonds. The theoretical *GD* can be from 20 to 67 wt% hydrogen adsorption, which is greater than $Li^{3}H$/LiH.[10] The most novel hydrogen storage candidate is graphane, fully hydrogenated graphene. Graphane is not reactive in water or air; it has theoretical higher mechanical and thermal strength than graphene. The diamond crystal lattice structure makes the carrier extremely stable in harsh environments.[11] The graphane-

like nanofiber carrier system has a *GD* of 17 wt% hydrogen.[12] The disadvantages are difficulties in fabrication from single layer to micro system and keeping the *GD* constant with any decrease. Most importantly, these structures have not been tritiated or deuterated yet. Hydrogenation and deuteration with reproducibility must be established before tritiation should be performed.

Graphene has also been tested as a hydrogen storage system using physisorption. Zhu and Li[13] at the University of Maryland, College Park, have demonstrated hydrogenation-assisted graphene origami (HAGO) as a hydrogen storage system using vdW to fold graphene, as well as stabilizing the folded nanostructure against the perturbation from thermal fluctuation. Through molecular dynamic simulations, they have demonstrated a feasible and robust HAGO process. The graphene nanocage can be opened and closed in a programmable fashion with control of an external electric field. This allows controllable molecular mass uptake, storage, and release, as well as high-density hydrogen storage. The hydrogen storage density using a graphene nanocage depends on the nanocage size, which is very linear. In summary, graphene nanocage can stably store hydrogen molecules with a weighted percentage of 9.7 wt% H_2 (18.4 wt% of H), but the nanostructure is still not fully hydrogenated.[13] The most promising carbon form is a hybrid form between CNTs and graphane called graphane-like nanostructure. These carbon nanostructures, including carbon aerogels such as activated porous carbon, show promising potential in hydrogen and tritium storages as a high-density energy source for short- and long-term applications.[14]

1.1 Tritium Compound Metrics

Tritiated compound metrics are collected and calculated for direct comparison. (See Appendix A for equations and assumptions). There are 2 figure of merits (FOM_{2DS}) for planar (2-D) configuration: input beta-flux power (dP_β/dS) and effective surface activity (S_m) exiting the planar source surface. These metrics are measured or calculated at the saturation point limited by self-absorption of layer. The mass absorption coefficient μ_m, in units of square centimeters per gram, is based on empirical data from titanium tritide-based sources (shown in Appendix A, Eq. A-3).[7,8] Each model is slightly different depending on the radiation source and elements used. This is typical for calculating mass absorption coefficients. In this report, Bower's μ_m is used to calculate the tritiated compound parameters shown in Table 1.[7,8]

Beta-flux power, also called power density, is calculated from the point source dose function for thin-layer sources (see Appendix A).[7,8] The beta-flux power, dP_β/dS, is influenced by the parameter η_β, which characterizes the efficiency of conversion

of beta particle energy in the decay into the beta flux exiting the surface of the thin layer. Bower et al.[7] sets the parameter constant for the tritiated compound calculation at 17% for saturation layer thickness ($D_{0.99}$). For some tritiated compounds, both FOM_{2D}'s are measured using a surface activity monitor.[1,7,8] Based on published research, tritiated metal hydrides have the highest FOM_{2D}'s.[1,7,8] Other potential candidates such as carbon nanostructures also show promise. However, graphene and CNT hydrogenation and deuteration have not yet been fully mastered or controlled. Further development is necessary before carbon nanostructure tritiation.

1.2 Tritium-Substituted Nitroxide

The most promising approach to fulfill the near-term goal of approximately 30 mCi/cm^2 from a single side of a thin layer is tritiating a compound that has low mass density ($\rho_m \approx 0.1$ g/cm^3) and low molecular weight but comparable GD and A_m to tritiated metal hydrides greater than 10 wt% ^{3}H and 1,000 Ci/g. The compound, having a greater beta penetration depth, can allow a greater beta-flux power to reach the semiconductor depletion region. The compound needs to have the ability to coat different aspect ratio semiconductor surfaces (nano- or micro-pillars, honeycomb, whiskers, etc.) and be used in both betavoltaic cells.

This report explains the usages and tritiation of nitroxides for betavoltaic cell applications. Calculations are formulated to compare with existing tritiated metal hydrides following Bower et al.[7] In addition to the theoretical calculations, ESTAR and MCNPX are used to model a planar configuration. Model FOM_{2D}'s are compared to theoretical calculation values. As a proof of concept, we describe the tritiation of a nitroxide, as a beta source for electrical driven devices shown in Fig. 1. We consider this synthesis and tritiation Scheme 1. We have chosen nitroxides, specifically nitroxide radical tetramethyl-1-piperidinyloxyl (TEMPO), to accumulate tritium for several reasons. First, these paramagnetic compounds are incredibly stable, some lasting at least 40 years without decomposition when unlabeled with tritium. Such long stability will allow us to assess the stability of tritiation on these compounds. Second, nitroxides are typically synthesized as 6- and 5-membered rings. The preparation of a 6-membered ring is depicted in Fig. 1, where functional groups allow ease of the addition of tritium to the molecule. Fourth, these nitroxides have low molecular weights compared to tritiated polymers, and they are solids at ambient STP conditions, allowing them to be easily attached to various surfaces. Tritium outgassing and compound degradation for one tritiated nitroxide type are measured for less than a month in solution and solid form.

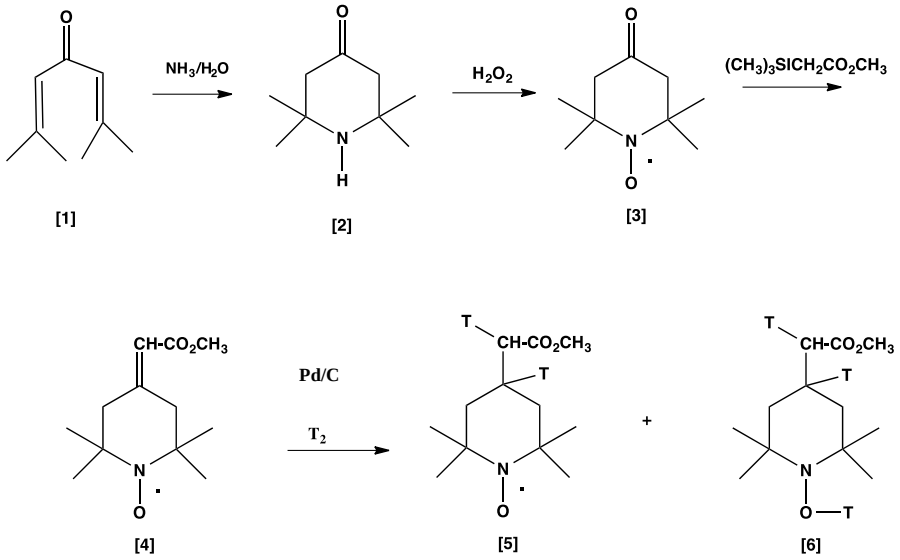

Fig. 1 Scheme 1 skeletal model of precursor (4) synthesis and tritiation process. Steps (1–4) are synthesized by Organic Electronic Devices LLC (OED LLC). The precursor (4) is tritiated using catalyst and tritium gas (^{3}H = T) by ViTrax LLC. If compound (6) is not held at vacuum and exposed to air, it will lose one tritium leaving a free electron (5).

2. Nitroxide: Tritiation Procedures, Calculations, and Modeling

Four types of nitroxides are selected to be tritium-labeled compounds. The nitroxide product for each synthesis is shown and labeled in Fig. 2. The mass density of each compound has not been measured. We predict that the nitroxide will have a mass density of approximately 0.1 g/cm^3. This report discusses the outcome of the tritiated nitroxide radical TEMPO shown in Fig. 3a (5, 6) and Fig. 1 (5, 6) as Compound 1, which is a proof of concept for all tritium-substituted nitroxides. The other selected compounds will be tritiated after further stability measurements of tritiated Compound 1. Compounds 2, 3, and 4 have been completely deuterated as a sensitive probe for electron paramagnetic resonance imaging.[19–23] We explain the procedure and theoretical tritiation values for each compound based on equations and assumptions from Bower et al.[7] These values are calculated by substituting the hydrogen and deuterium synthesis with tritium.

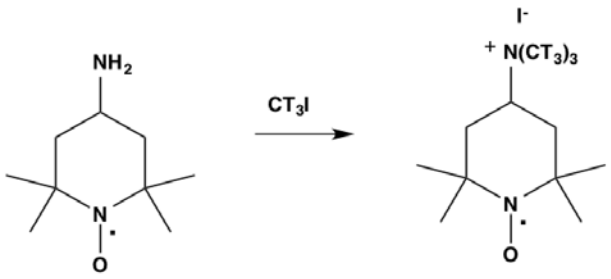

Fig. 2 Tritiation process of Compound 3 (Scheme 3) with tritiated methyl iodine precursor

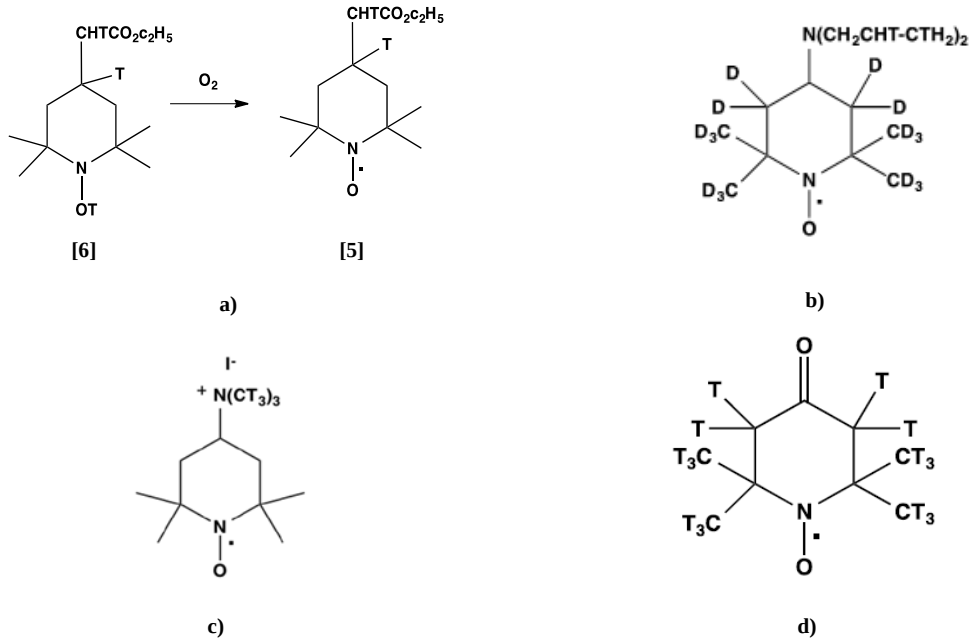

Fig. 3 Tritiated nitroxide products: a) tritiated 4-methoxycarbonyl-methylene-2,2,6,6 tetramethyl-1-piperidinyloxyl (Compound 1), b) tritiated 4 methoxycarbonyl-methylene-2,2,6,6-tetramethyl-1-piperidinyloxyl using reductive amination (Compound 2), c) N,N,N-trimethyl ($^3H_9$)-2,2,6,6-tetramethyl-1 piperidinyloxyl iodide (Compound 3), and d) 4-oxo-2,2,6,6-tetra($^3H_3$)methyl (3,3,5,5-$^3H_6$)piperidinyloxyl (Compound 4)

2.1 Tritium Procedures and Theoretical Calculations

Tritiated 4-methoxycarbonyl-methylene-2,2,6,6-tetramethyl-1-piperidinyloxyl (M = 235 g/mol), Compound 1, is the first compound to be tritiated by ViTrax.[24] It requires a 1-step synthesis using tritium gas and catalyst. The precursor synthesis and tritiation are explained in Section 3. Compound 1 precursor has been hydrogenated and deuterated for electron paramagnetic resonance imaging (Fig. 1 [4]). The theoretical tritium gravimetric density ($\underline{GD}$) is 3.98 wt% ^{3}H. If the sample is held under vacuum, 3 tritium atoms are bonded to the nitroxide. When the sample is not held in vacuum and exposed to air, the tritium atom bonded to the oxygen on the 6-membered ring will be lost, giving way to a free electron. The specific activity (A_m) at 380 Ci/g is greater than ^{3}H gas, but the dP_β/dS of 0.34 $\mu W_n/cm^2$ (9.5 mCi/cm^2 based on an average electron energy of 5.7 keV) prohibits it from being an adequate substitute for current solid ^{3}H sources or ^{3}H gas at STP (Tables 1 and 2).

Table 2 Theoretical calculations of tritiated nitroxides. FOM_{2D}'s account for one side of the tritiated layer. Parameters are calculated using equations in Bower et al.[7]

Tritiated compound type	Specific activity (A_m) (Ci/g)	Mass density (ρ_m); (g/cm^3)	Gravimetric density (GD) (wt% ^{3}H)	Volume activity (V_m) (Ci/cm^3)	FOM_{2D} specific beta-flux power at $D_{0.99}$ ($\frac{dP_\beta}{dS}$); [$\frac{\mu W_n}{cm^2}$]	Beta range depth (D_L)[a,b] (μm)	FOM_{2D} effective surface activity (S_m) (mCi/cm^2)
Compound 1	379	0.1	4	38	0.341	9.5[a,b]	10
Compound 2	583	0.1	5.7	58	0.525	11[a,b]	15
Compound 3	824	0.1	9	82	0.741	13[a,b]	21
Compound 4 step **(2)**	2526	0.1	26	253	2.27	10[a,b]	67
Compound 4 step **(3)**	2371	0.1	25	237	2.13	10[a,b]	63

[a] Layer thickness (D_L) for betavoltaic cell following Thomas et al.[1] approach.
[b] Beta range depth is calculated from ESTAR[18] and following the process used in Thomas et al.[1] ESTAR calculations at average ^{3}H beta energy of 5.7 keV.[18] Equations shown in Appendix A.

Tritiated 4-methoxycarbonyl-methylene-2,2,6,6-tetramethyl-1-piperidinyloxyl (M = 261 g/mol), Compound 2, using reductive amination is the second tritiation candidate, Fig. 4. Compound 2 precursor, Fig. 4 (4a) and (7), like Compound 1, has been hydrogenated and deuterated. Compound 2 tritiation also requires 1-step synthesis.[20,21] If tritiated, it consists of 4 to 5 tritium atoms. The fifth tritium atom requires the compound to be held under vacuum after synthesis. The tritium atom is bonded to the oxygen on the 6-membered ring in an identical to Compound 1.

The volume activity, surface activity, and dP_β/dS are greater than Compound 1. The maximum specific beta flux is approximately 0.5 $\mu W_n/cm^2$ (15 mCi/cm^2 based on an average electron energy of 5.7 keV). Compound 2 synthesis will allow us to identify the initial 24-h stability and yield percentage when more than 3 tritium atoms are bonded to the nitroxide (NO_x) 6-membered ring.

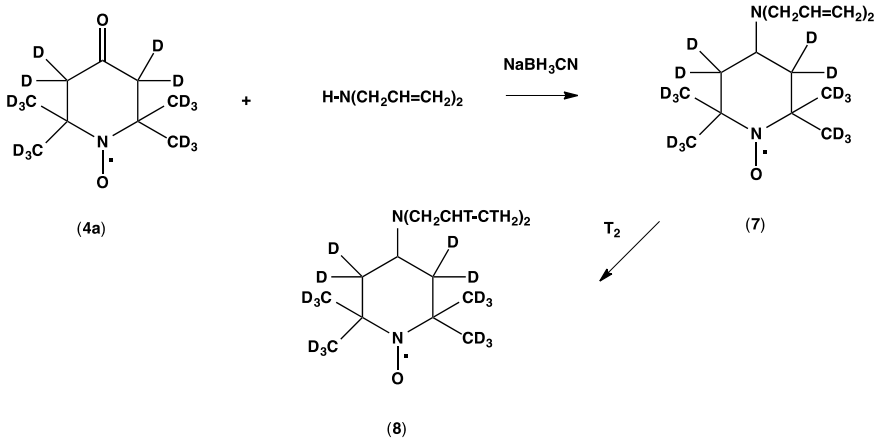

Fig. 4 Tritiation of Compound 2 using reductive amination (Scheme 2) is shown in schematic. An additional tritium atom could be bonded to the oxygen with the free electron if the sample is synthesized under vacuum.

N,N,N-trimethyl ($^3H_9$)-2,2,6,6-tetramethyl-1-piperidinyloxyl iodide (*M* = 347 g/mol), Compound 3, is the third tritium carrier compound (Fig. 2). Compound 3 tritiation synthesis follows Rosen et al.[22] and Eriksson et al.[23] procedures. Tritiated methyl iodide, which is commercially available, is added to a solution of dimethylformamide, DMF, (5 mL) of 4-amino-2,2,6,6-tetramethyl-1-piperidinyloxyl, Fig. 2 (1), (0.17 g, 1 mmol) and 4-hydroxy-2,2,6,6-tetramethyl-piperidine (0.31 g, 2 mmol, Aldrich) at room temperature. The mixture is stirred until it becomes homogenous and then the solution is allowed to stand for 3 h at room temperature. Crystals form, which are then filtered, and washed with diethyl ether giving tritiated nitroxide, Fig. 2 (2). The synthesis yield is 50% when hydrogenated. Compound 3 is an improvement to the previous 2 compounds with respect to greater beta-flux power of 0.7 $\mu W_n/cm^2$ (21 mCi/cm^2 based on an average electron energy of 5.7 keV) and 9 tritium atoms in total.

Compound 4 in this report, 4-oxo-2,2,6,6-tetra($^3H_3$)methyl-(3,3,5,5-$^3H_6$)piperidinyloxyl (*M* = 205 g/mol), is the fourth and final tritium carrier compound that will be potentially tritiated. Tritium synthesis is a 2-step process following Burks et al. [19] (Fig. 5). Ammonium chloride (3.5 g, 65 mmol) is added to a 250-mL round bottom flask containing oven-dried anhydrous sodium carbonate (3.18 g, 30 mmol) and magnesium oxide (3 g, 75 mmol). Then, tritium-substituted

acetone, Fig. 5 (1), (20 mL) is introduced into the flask. After sealing the flask with a rubber septum, the reaction is heated to 50 °C in an oil bath for 3 days. Upon cooling, diethyl ether is added to the resulting solid. It is filtered, and then the filter cake is crushed into a fine powder washed with diethyl ether and filtered. This procedure is repeated 2 more times.

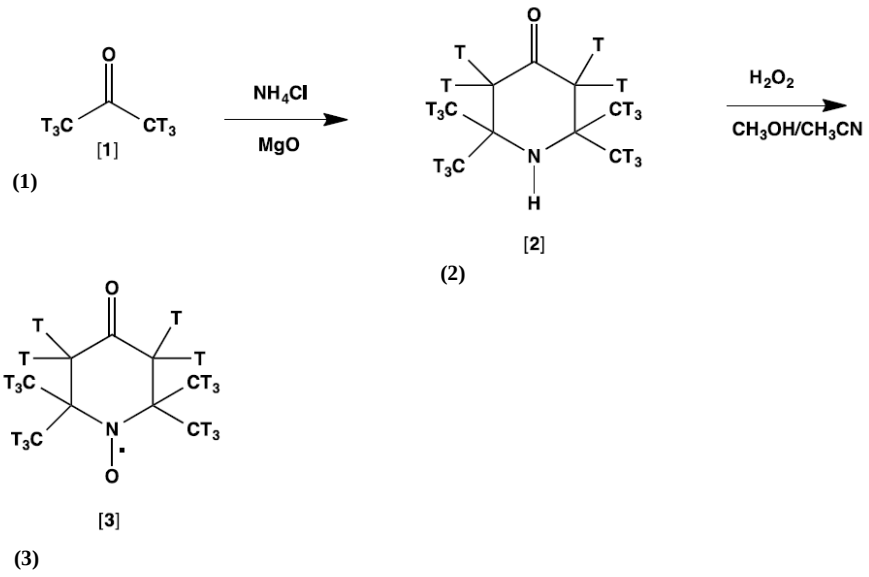

Fig. 5 Tritiation process of Compound 4 (Scheme 4) with tritiated acetone precursor

The combined filtrates are evaporated to dryness in vacuo, affording a red liquid (5.35 g), 4-oxo-2,2,6,6-tetra($^3H_3$)methyl-(3,3,5,5-$^3H_6$)piperidine (Fig. 5 [2]). A solution of crude 4-oxo-2,2,6,6-tetra($^3H_3$)methyl-(3,3,5,5-$^3H_6$)piperidine, (5.35 g, 2.86 mmol) dissolved in a mixture of methanol (35 mL) and acetonitrile (10 mL), is added to sodium hydrogen carbonate (2 g) and sodium tungstate (0.29 g). Then, hydrogen peroxide (30%, 11 mL) is added, and the mixture is kept at room temperature for 2 days. Next, the reaction is filtered with a saturated solution of sodium chloride (100 mL). Extraction with diethyl ether is afforded, after drying with anhydrous magnesium sulfate, crude 4-oxo-2,2,6,6-tetra($^3H_3$)methyl-(3,3,5,5-$^3H_6$)piperidinyloxyl (Fig. 5 [3]). This compound is chromatographed, eluting with hexane/diethyl ether (4:1) to yield pure 4-oxo-2,2,6,6-tetra($^3H_3$)methyl-(3,3,5,5-$^3H_6$)piperidinyloxyl, as red oil that solidified upon standing (2.9 g, 51%).[19] If stable during tritiation procedure, Compound 4 *FOM*$_{2D}$'s from theoretical calculations surpass near-term goals with a beta-flux power of 2.27 $\mu W_n/cm^2$ (67 mCi/cm^2 based on an average electron energy of 5.7 keV) and 16 tritium atoms bonded to the monomer.

For all nitroxides, the surface activity is heavily dependent on the synthesis yield and available tritium quantity. After tritiation and high-performance liquid chromatography (HPLC), the tritiated compound can be purified using a column technique. Further testing is required to understand the correlation between deuteration and tritiation yield and overall stability during synthesis. In addition, there is still concern that the compound might breakdown during or immediately after tritiation because of a high number of tritium atoms bonded to the 6-membered ring. Extra care immediately after tritiation might be required to store the compound in activated porous carbon or a solution such as toluene in case of compound degradation and ^{3}H outgassing. As long as the compound is stable during synthesis without much tritium outgassing, a technique will be developed to seal the compound on the semiconductor substrate immediately after tritiation is completed.

2.2 ESTAR and MCNPX Modeling

The Continuously Slowing Down Approximation using National Institute of Standards and Technology ESTAR software is used to approximate the electron range in compounds for monoenergetic electron energies. The input parameters are mass density, compound formula, and relative weights.[18] The average beta energy of ^{3}H used for the model is 5.7 keV. To confirm the accuracy of ESTAR electron range, tritiated metal hydride parameters are inserted in model. The electron range for titanium tritide is 532 nm at 5.7 keV. In Thomas et al., the optimal (before beta-flux saturation point) metal foil thickness is 400 nm for ^{3}H beta spectrum, which is 25% less than the ESTAR electron range thickness.[1] For the nitroxide compounds electron range, this factor is accounted for to give an optimal layer thickness range of 10–13 μm (Table 2).

ESTAR is a simple 1-D model that only identifies the 100% electron stopping range of a monoenergetic electron energy. MCNPX can generate a more realistic model using more than one dimension, electron energy spectrum, isotropic source irradiation option, and energy deposition profiles in structures. MCNPX is a general purpose Monte Carlo code that has the capability to model neutron, photon, and electron (or coupled) transport. The software can simulate transportation of particles with energy from 1 keV to 100 MeV in materials. The model is based on axial symmetry, reducing 3-D structures into a 2-D configuration. There are 3 main cylinder components in order of placement: nitroxide compound, tritiated nitroxide compound (tritium filled in nitroxide volume), and gallium nitride (GaN) bulk structure (Fig. 6). The nitroxide compound is 100 μm thick with a 1-cm^2 area. The tritiated nitroxide thickness ranges from 5–200 μm with an area of 1 cm^2. The molecular weight is 176 g/mol consisting of 3 tritium atoms bonded to monomer with mass density of 0.1 g/cm^3. The GaN thickness is 100 μm with a 1-cm^2 area.

GaN structure is the selected semiconductor in the betavoltaic cell. The nitroxide volume is divided into 5-µm layers; GaN volume is divided into 100-nm layers. Energy deposition profiles are formulated and energy percentages exiting the tritiated nitroxide volume space into the nitroxide and GaN space are calculated (Figs. 7 and 8).

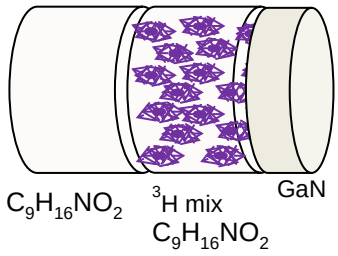

Fig. 6 Planar model in MCNPX; purple symbols represent the isotropic beta emission in the nitroxide volume

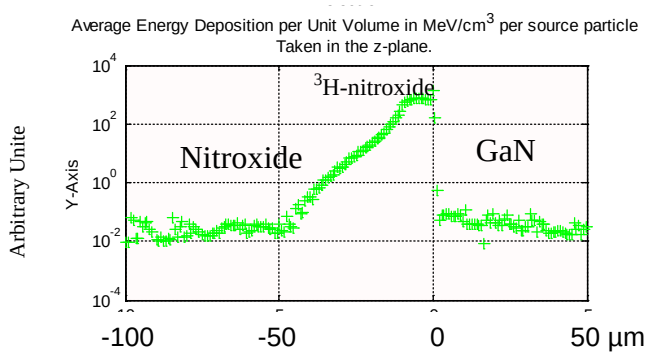

Fig. 7 Energy deposition profile as a function of layer thickness. In this profile, the ^{3}H-nitroxide is 10 µm, GaN is 100 µm, and nitroxide is 100 µm thick. ^{3}H-nitroxide is surrounded on both sides to confirm conservation of energy.

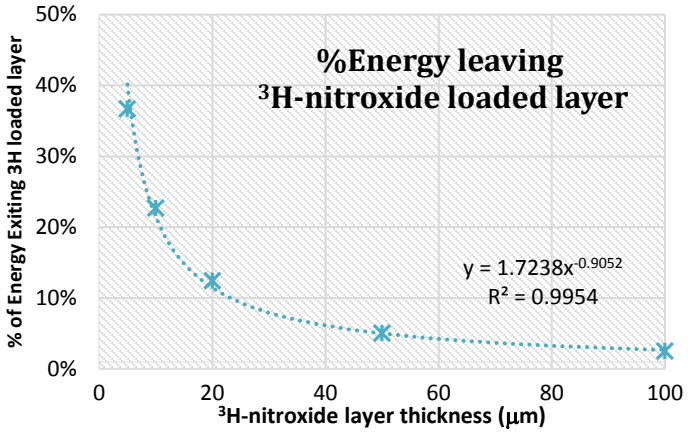

Fig. 8 Energy percentage exiting ^{3}H-nitroxide surface as function of ^{3}H nitroxide layer thickness. The energy percentage of tritiated volume accounts for both sides of the layer.

Energy deposition profiles show that all tritium beta energy is stopped within 1.5 µm of GaN and 50 µm of untritiated nitroxide. If GaN structures surrounded the tritiated nitroxide layer with a thickness of 20 µm on both sides, 12% of total beta energy is deposited within 100 nm, which would reach the GaN depletion region in reference to actual GaN betavoltaic devices. Total specific activity is calculated for the nitroxide volume in Appendix B for relevant calculations. The optimal thickness with S_m of approximately 6 mCi/cm^2 and dP_β/dS of approximately 0.2 µW$_n$/cm^2 is 20 µm. These FOM_{2D}'s account for a single side of the tritiated layer. To reach at least 20 mCi/cm^2 for a single layer side, we would need at least 9 tritium atoms in the nitroxide compound. This set goal is necessary to be comparable to published metal hydride S_m values. Nevertheless, when projecting in 3-D, the nitroxide has a few advantages over the metal hydride such as using beta emission from more than one side and conformal coating on various semiconductor structures. A 1-D MCNPX model of Ti^{3}H$_2$ is formulated to check the ^{3}H-nitroxide model validity (Appendix B). The Ti^{3}H$_2$ model FOM_{2D}'s are greater than Bower's calculations and experimental results, S_m is 40 mCi/cm^2 for a single side with a layer thickness of 400 nm. The percent of energy leaving the tritium-loaded layer is 23%. If the layer is only 80% loaded, then the S_m is 32 mCi/cm^2. This value is 25% larger than theoretical value at 24 mCi/cm^2. This significant difference between the model and theoretical results limits the soundness of the ^{3}H-nitroxide model results.

3. Tritiation and Stability Measurements of 4-Methoxycarbonyl-methylene-2,2,6,6-tetramethyl-1-piperidinyloxyl (Compound 1)

4-Methoxycarbonyl-methylene-2,2,6,6-tetramethyl-1-piperidinyloxyl (Fig. 1 [4]) is tritiated to measure the yield percentage and stability of the tritium synthesis (Fig. 1). A quantity of 100 mg of precursor (Fig. 1 [4]) is prepared to be tritiated by ViTrax LLC. Mass spectroscopy analysis is performed on the precursor to identify the compound shown in Fig. 9. Purity of the precursor is assessed by HPLC (Fig. 10) and is described in Appendix C. The photodiode array (PDA) chromatogram shows only one peak, indicating the precursor sample has high purity. Tritium reduction reaction with approximately 2 mg of precursor is placed in glass vessel filled with 100 mCi of tritium gas. Palladium on carbon is used for catalytic tritiation of precursor (Fig. 1 [4]), in a 1-step process. The crude solution is filtered, and then co-evaporated several times with a protic solvent to remove all labile tritium. The crude product (Fig. 1 [5, 6]), is dissolved in toluene and assayed for total activity. It is stored at –20°C and 1 atm. The toluene serves 2 experimental purposes: a stable median for the radio-labeled compound and an HPLC solvent. Figure 1 shows the synthesis and tritiation of 4-methoxycarbonyl-methylene-2,2,6,6-tetramethyl-1-piperidinyloxyl (Fig. 1 [4]) process performed by OED LLC and ViTrax.

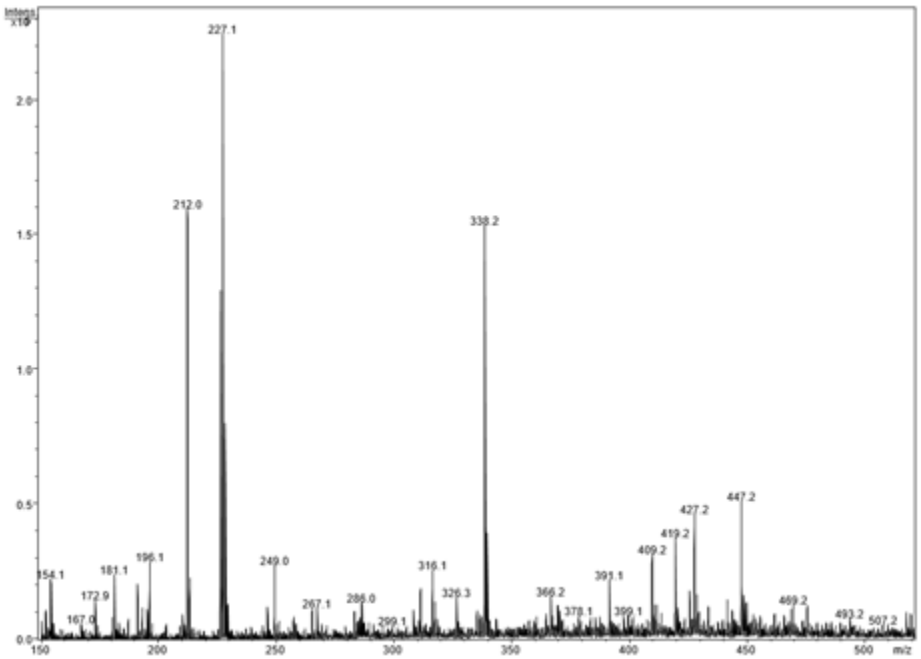

Fig. 9 Mass spectrum of precursor sent to ViTrax. Positive ion mode: $(M+H)^+$ (m/z 227.1), $C_{12}H_{20}NO_3$ = 226.3 g/mol.

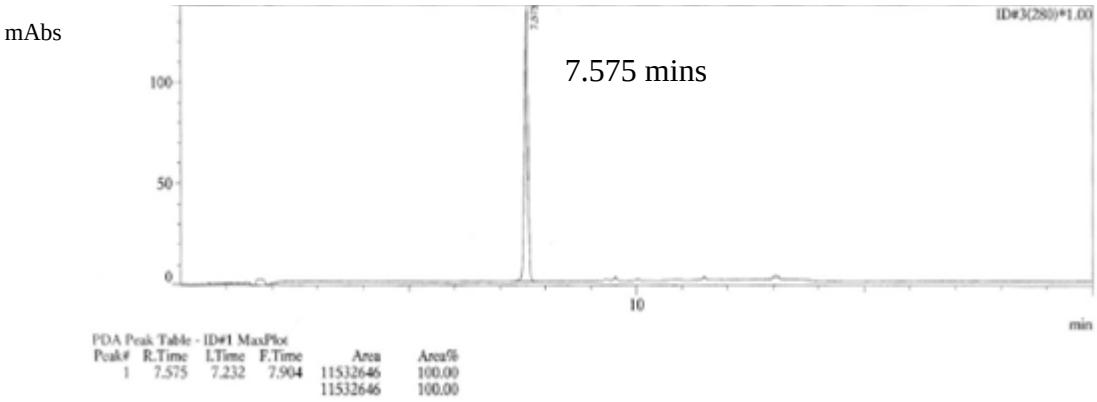

Fig. 10 A PDA chromatogram of precursor (Fig. 1 [4]), obtained by HPLC analysis to measure precursor purity. The 7.575-min retention time peak (x-axis) represents the precursor. The y-axis (mAbs) is the milli-absorbance units measured by the PDA. There is no other retention time, which proves there is only one compound type and high sample purity.

A crude yield of 86 mCi is prepared via catalytic reduction of a double bond. The rest of tritium did not bond to the sample. The specific activity obtained via mass spectroscopy analysis (Fig. 11) is approximately 25 Ci/mmol (A_m = 103 Ci/g). The experimental specific activity is limited by available tritium during radioisotope labeling, representing 28% of the maximum loading of the compound. Typically, for a double bond reduction, between 40 and 50 Ci/mmol is obtained. It is suspected that some tritium alpha is being lost to the ester bonded to the side group of the nitroxide radical TEMPO 6-membered ring. The ester-cleaved product is detectable and is used to assess the specific activity. The tritiated compound is measured by HPLC again for detection of other compound types in the sample. The HPLC profile of the crude reduction product has 2 very distinct retention times, which means that the sample has 2 types of compounds. Retention time is the time from the injection of the sample (analyte) to the identification by the detector (PDA). We are confident, based on retention times, that the peaks at 7.65 and 1.729 min (Fig. 12) identify the desired product, tritiated hydroxylamine, and the cleaved ester, (Fig. 1 [5, 6]), respectively, in the toluene solution. Compound 1 (Fig. 1 [6]) has a lower retention time because it is a nonpolar molecule passing more quickly through the stationary phase in the column. Retention time at 7.65 min is greater than precursor retention time at 7.575 min with an increase of molecular weight because of the additional 3 tritium atoms. The retention time of compound 5 in Fig. 1 is greater because it binds/adsorbs to the silica due to polarity. The 1.729-min peak is compound 6. The 1.729-min peak has a shoulder portion, which could be cleaved ester (side group, $C_3H_4O_2{}^3H$) due to beta decay. This portion could include the broken up tritiated nitroxide compound. Figures 11 and 12 show plots of the mass spectrum and HPLC profile, respectively.

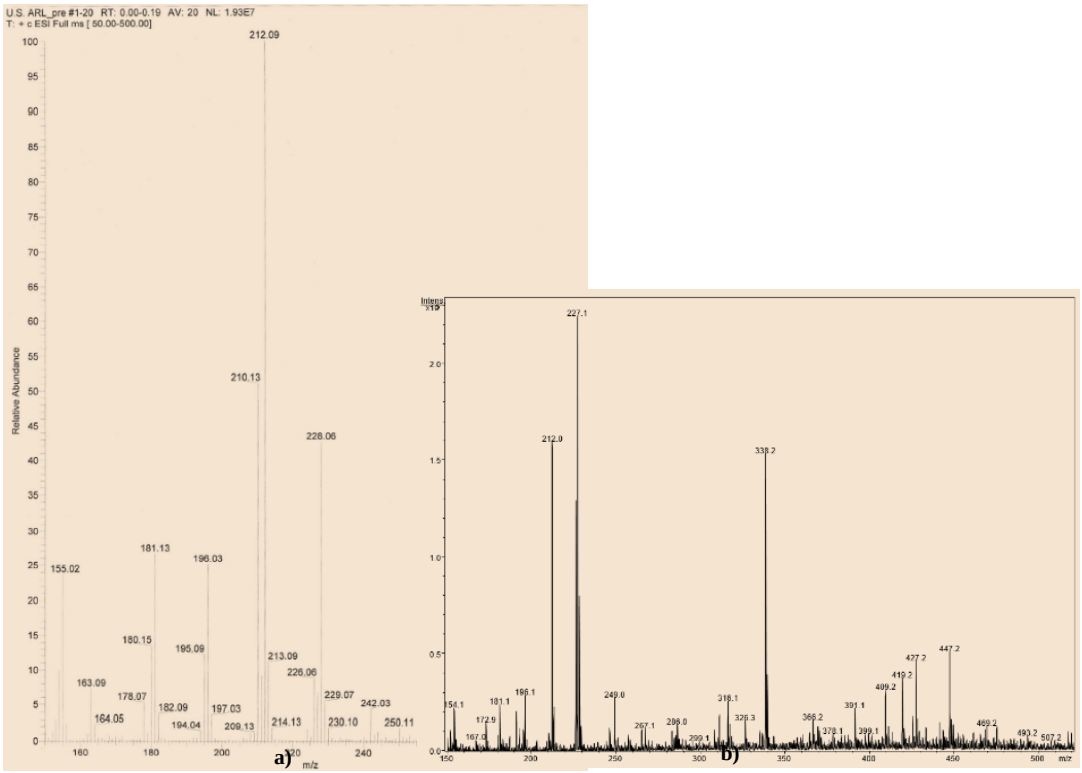

Fig. 11 Mass spectrum of a) tritiated 4-methoxycarbonyl-methylene-2,2,6,6 tetramethyl-1-piperidinyloxyl, tritiated hydroxylamine (Fig. 1 [5, 6]) and ester side group done by ViTrax and b) precursor (Fig. 1 [4]) done by OED LLC

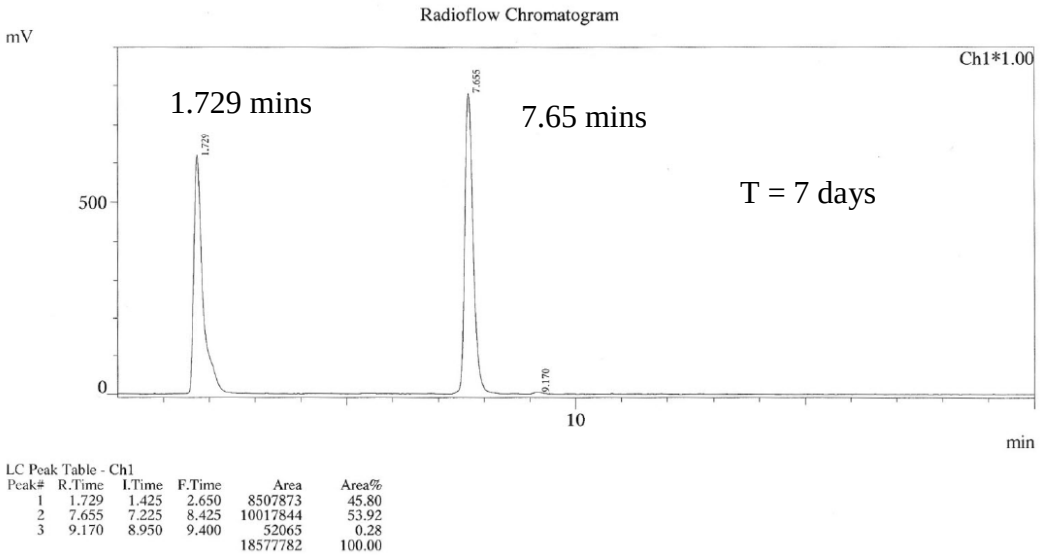

LC Peak Table - Ch1

Peak#	R.Time	I.Time	F.Time	Area	Area%
1	1.729	1.425	2.650	8507873	45.80
2	7.655	7.225	8.425	10017844	53.92
3	9.170	8.950	9.400	52065	0.28
				18577782	100.00

Fig. 12 A radio flow chromatogram of the tritiation of nitroxide (Fig. 1 [4]) by HPLC analysis. There are now 2 different retention lines after tritiation. The peaks at 7.65 and 1.729 min represent the desired tritiated product (Fig. 1 [5]) and cleaved ester (side group, $C_3H_4O_2{}^3H$) compound (Fig. 1 [6]) in the toluene solution. We are not able to distinguish if the compound loses or gains a tritium atom bonded to the oxygen on the ring because of storage environment. The x-axis is retention time (min) and y-axis is in millivolt units.

The precursor is tritiated and considered initially stable for at least 24 h using a 1-step synthesis in solution form. Since the compound is stable in toluene for more than 24 h, ViTrax could perform mass spectroscopy and HPLC. To further our understanding of nitroxide degradation from primary and secondary irradiation effects, the stability of this mixture is assessed for both tritium lability and HPLC composition change in solution and solid form. The percent retention of tritium is shown in Table 3 and the HPLC profiles are shown in Fig. 13.

Table 3 Tritium content in the sample. For solution forms, the sample is initially dissolved in toluene where it stays during the entire experiment (T = 1–27 days).

Sample: Compound 1	^{3}H% content (%)
Solution T = 1 day	100
Solution T = 7 days	100
Solution T = 27 days	100
Solid T = 7 days	53
Solid T = 14 days	58
Solid T = 21 days	55

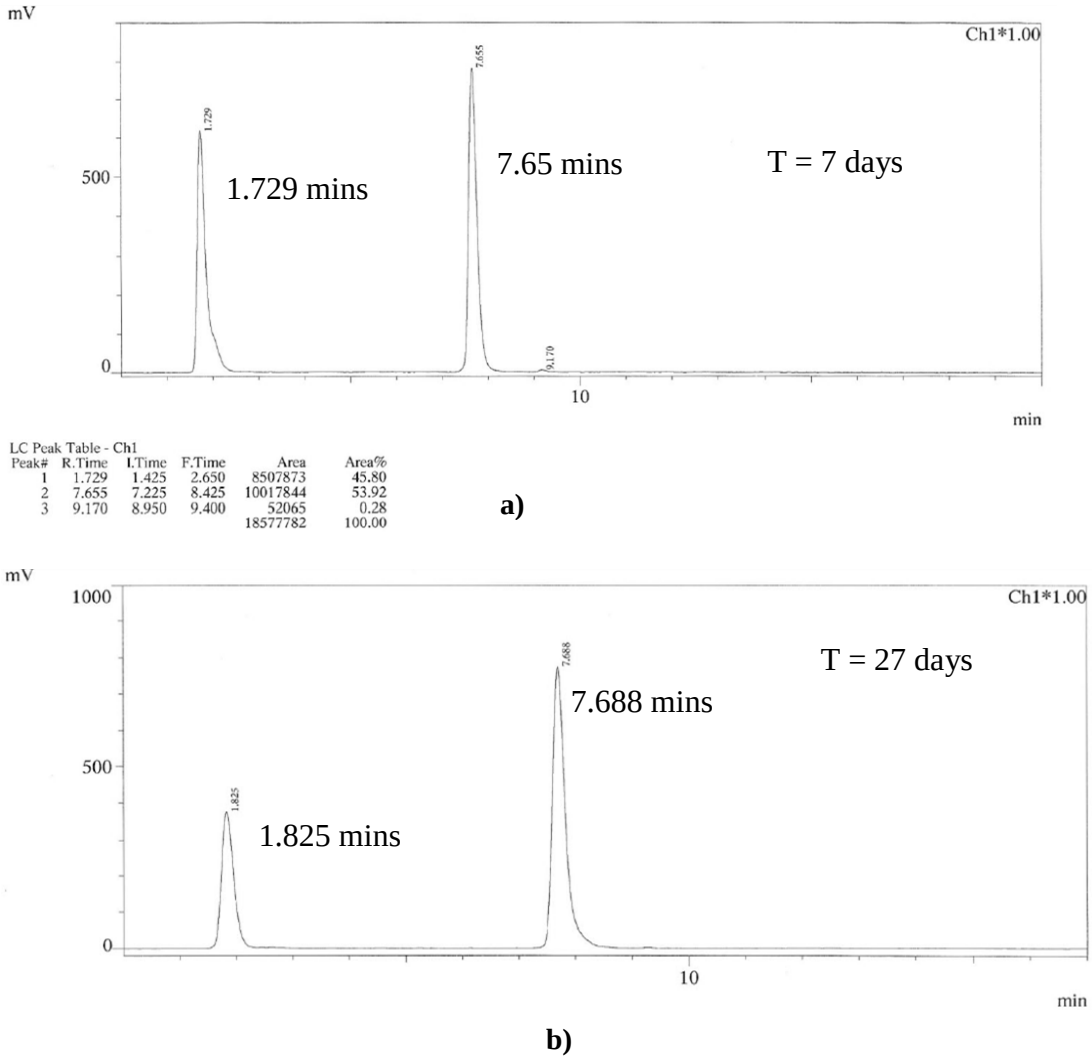

Fig. 13 A radio flow chromatogram of compound 5 (7.688 min) and cleaved ester and compound 6 (1.825 min) obtained by HPLC analysis. There are still 2 different retention lines after tritiation at a) T = 7 days and b) T = 27 days. The compound in solution form is completely stable with little or no degradation or tritium loss after 27 days. The x-axis is retention time (min) and y-axis is in millivolt units.

When stored at –20°C, the solution form in toluene appears stable after 27 days based on HPLC analysis showing an absence of tritium lability (Fig. 13). After Day 27 of solution measurement, three 8-mCi dry samples from the leftover supply are prepared from the toluene solution and analyzed for stability at Day 7, 14, and 21. The 3 samples are stored at STP. The solid stability based on HPLC profiles is low with what appears to be nearly complete loss of the retention time peak at 7.6 min (Fig. 14). There are additional peaks in the profile, which means that other compounds are being formed due to degradation and tritium loss. Tritiated hydroxylamine (Fig. 1 [5]), at 7.65 min, starts reducing in intensity as other retention times are appearing. The cleaved ester and Compound 1 (Fig. 1 [6]), with

a retention time of 1.82 min is still well defined and does not lose intensity. Tritium lability is at approximately 50% at Day 7. It appears that tritium lability saturates at Day 7 with minimal loss at Days 14 and 21. The tritium loss saturates at 55 ± 2.5%. Figure 15 shows a plot of the tritium loss as function time for solution and solid form.

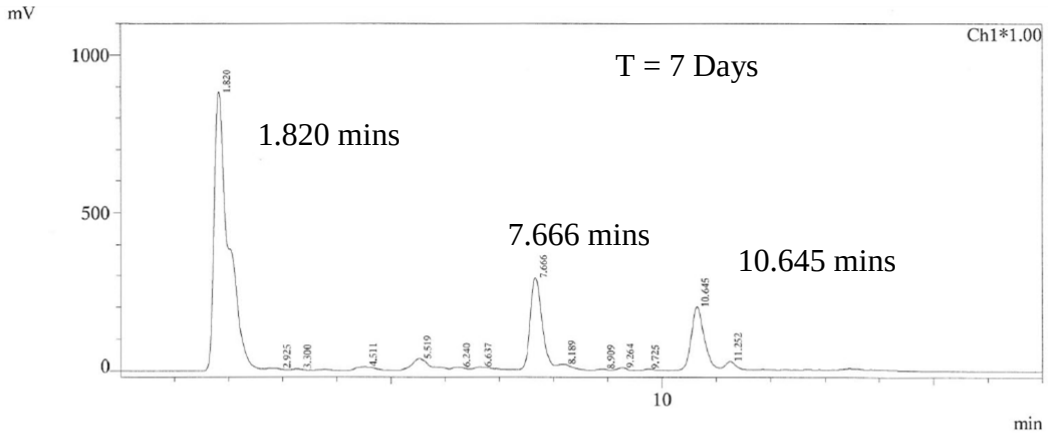

LC Peak Table - Ch1

Peak#	R.Time	I.Time	F.Time	Area	Area%
1	1.820	1.525	2.675	16342793	61.18
2	2.925	2.675	3.075	112839	0.42
3	3.300	3.075	3.475	51111	0.19
4	4.511	4.100	4.950	285219	1.07
5	5.519	4.950	6.075	863652	3.23
6	6.240	6.075	6.450	166856	0.62
7	6.637	6.450	7.175	279803	1.05
8	7.666	7.175	8.050	4480866	16.78
9	8.189	8.050	8.675	359199	1.34
10	8.909	8.675	9.050	55383	0.21
11	9.264	9.050	9.550	99770	0.37
12	9.725	9.550	10.300	48267	0.18
13	10.645	10.300	11.075	3211400	12.02
14	11.252	11.075	11.750	353973	1.33
				26711132	100.00

Fig. 14 A radio flow chromatogram of tritiated hydroxylamine (Fig. 1 [5]), (7.666 min) and cleaved ester and compound shown in Fig. 1 [6] (1.820 min) obtained by HPLC analysis at T = 7 days. An additional peak is shown in the profile, which means that other compounds are being formed due to degradation and tritium loss. Tritiated hydroxylamine (Fig. 1 [5]), at 7.666 min, starts reducing in intensity as other retention times are appearing and increasing.

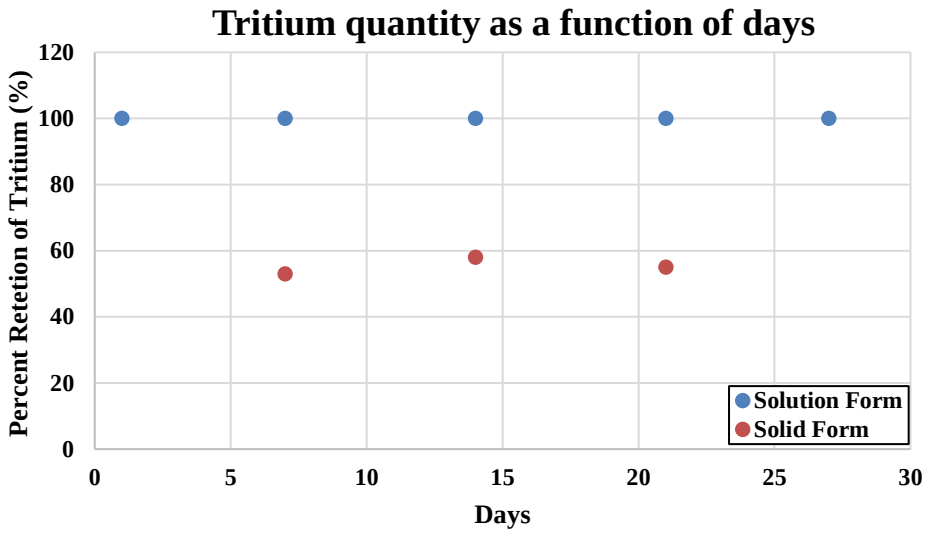

Fig. 15 Plot of tritium percentage quantity accrued in sample (tritiated hydroxylamine, ester, and broken-up tritiated nitroxide group) as function of days. Solution form has nearly zero tritium loss whereas the solid sample losses 50% of its tritium before plateauing after 7 days. Each data point is one sample for each day.

For the solution form, the concentration of ester and Compound 1 (Fig. 1 [6]) reduces from T = 7 days (at 1.729 min) to T = 27 days (at 1.825 min) (Fig. 13a and b). However, still only 2 retention times appear in the radio flow chromatogram, which shows that the ester and tritiated hydroxylamine are still stable (Figs. 12 and 13). For the solid form, tritiated hydroxylamine at retention time of 7.66 min reduces while the ester at 1.820 min stays constant at 61% of sample concentration after 7 days (Fig. 14). After 7 days, the shoulder is clearly defined on the 1.820-min peak. After 27 days, the 7.66-min intensity decreases to nearly zero and the ester concentration increases to nearly 80% of sample concentration. Tritium loss in the sample is approximately 50% in solid form compared to the solution form at nearly 100% due to stored conditions and radioactivity concentration (Fig. 15). It has not been confirmed if tritium is immediately lost during drying procedure from solution to solid form or during the week. The solution sample has to be heated to 120 °C to boil off toluene, leaving just the tritiated sample. Since the solid sample is stored at STP, exposure to air causes oxidation, producing free radicals and sample degradation. For primary beta-radiation effects, the solid form has a much greater concentration of tritium radioactivity versus the solution. Closer tritium proximity increases beta particle interaction with nitroxides without the toluene median. A single beta particle ejected due to decay can generate several diverse reactive species in the nitroxide compound. Primary radiation effects causes the cleaving of the ester initially bonded to 6-membered ring.

The results of solid and solution form stability are not surprising compare to other tritiated organic-based monomers and polymers. Tritium-labeled polymers have shown similar characteristics at specific activities greater than 10 Ci/g where the solid state is less stable than the liquid state.[8,25] An example of this relationship was done in the former USSR. ^{3}H-polystyrene manufactured as a solution had a specific activity of up to 50 Ci/g polymer, but in the solid state, the specific activity was only 2.5 Ci/g.[8,25] Up until now, previous research has shown limits of specific activity for monomers and polymers at 10 Ci/g. In the first trial, the tritiated nitroxide in solid form was already 5 times above that empirical limit.

4. Conclusion

Nitroxide compounds are identified as potential tritiated compounds for radioisotope batteries. Betavoltaic and betaphotovoltaic cells share similar drawbacks that limit source power density such as low-volume activity (Ci/cm^3), tritium gravimetric density (*GD* wt% ^{3}H), and geometric constraints (thin films) due to beta self-absorption. Nitroxides are selected as tritiated compounds because of low mass density, high deuteration and hydrogenation synthesis yield, high *GD* wt% ^{2}H and H (similar to tritiation process), and pliability to semiconductor structures (planar, nanopillars, etc.). Theoretical parameters are calculated for comparison with past and current tritiated compounds. One of the 4 selected compounds meets the short-term goal (S_m of thin layer ≥30 mCi/cm^2 from single side). An MCNPX model calculates a S_m of approximately 5.7 mCi/cm^2 for Compound 1 from one side of the 10-µm layer, which is nearly half the value of theoretical calculations based on Bower's[7] equations. There are differences between calculations due to the mass absorption coefficient and other parameters based on empirical equations for titanium tritide.

As a proof of concept, the nitroxide, 4-methoxycarbonyl-methylene-2,2,6,6-tetramethyl-1-piperidinyloxyl, is tritiated with a specific activity of 103 Ci/g in solution and solid form at approximately 86 mCi (Compound 1). Tritium stability measurements, both in solution and solid form, are executed to understand compound degradation and tritium loss as a function of time. The solution form in toluene is 100% stable after 27 days, whereas the solid form has 55 ± 2.5% tritium loss plateau after 7 days. Theoretical parameters of Compounds 3 and 4, high tritiation yield, and limited tritium loss of Compound 1 (solution and solid form) encourage further investigation and tritiation of nitroxide compounds to fulfill tritiated compound requirements.

5. Further Evaluation

Before we decide on tritiating another NO_x compound, it is necessary to construct a 2-D and 3-D model in MCNPX for other selected nitroxide compounds. We need to formulate an MCNPX model for metal hydrides such as tritiated titanium hydride and compare FOM_{2D}'s to published experimental results to confirm the 2-D model. For the 3-D model, a GaN structure with micropillar features (Fig. 16). The nitroxide compound will fill into the pillared device. Also, another model will have the tritiated nitroxide surrounded by the GaN structures (Fig. 17). Initial results from MCNPX modeling show that beta particles from 20-µm-thick layers penetrate the GaN layer. The proposed substrate design will have 10–20 µm high pillars with 20-µm trough/pillar separation. If we are able to fill the entire volume between these 3-D features, the tritiated nitroxide compound would be essentially surrounded by the semiconductor converter and vice versa; the key advantage over past beta sources is that betas can penetrate through the 20-µm-thick layer into the semiconductor for energy conversion. The S_m and dP_β/dS values from this 3-D model will be considered our new FOM_{3D}'s. These values will account for 6 faces of the tritiated compound cube. These values will be compared to past and present metal hydrides.

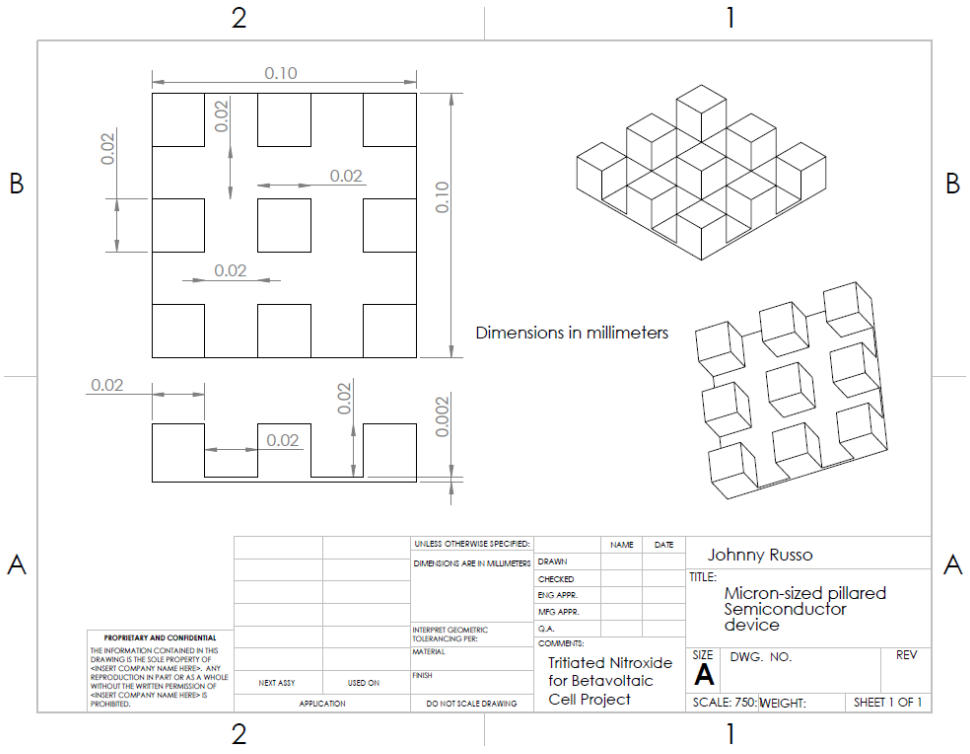

Fig. 16 Computer-aided design technical drawing of 3-D printed, etched, or grown micropillar structure (dimensions are in millimeters)

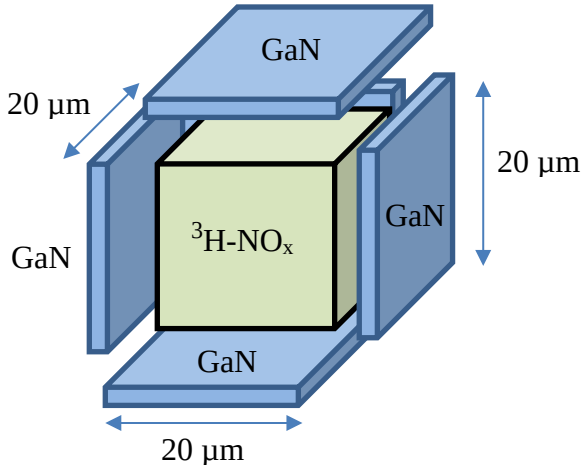

Fig. 17 Proposed 3-D MCNPX model to calculate new FOM$_{3D}$'s. The tritiated compound will be 20 × 20 × 20 µm. GaN surrounds tritiated nitroxide on all 6 sides of the tritiated compound cube.

In the initial phase of this program in which we exceeded all our goals, we were able to synthesize nitroxide (Fig. 1 [4]) when subjected to $^3H_2$ in toluene. Most remarkably, Compound 1 did not decompose in toluene for at least 27 days, and the experiment was terminated. While we lost approximately 50% of the tritium when the mixture was dried and exposed to air after 7 days, no further loss of radioactivity was measured over the course of 2 more weeks. Based on the success we have achieved, we will double and triple the tritium content through synthesis of Compounds 2, 3, and 4. We are confident that these compounds will be more stable than Compound 1 with respect to cleaving of the tritiated ester shown in HPLC plots. For example, with Compound 2 synthesis, we will double the tritium content by exposing nitroxide (Fig. 4 [4a]), to $^3H_2$ in toluene, while retaining a low molecular weight compound (Scheme 2) (Fig. 4). The design of nitroxide (Fig. 4 [7]), is based on 2 criteria. First, based on modeling, it appears that deuterium in place of hydrogen in the piperidine ring (Fig. 4 [4a]) enhances stability of a tritium-labeled nitroxide. Second, nitroxide, (Fig. 4 [8]) has double the tritium content of nitroxide (Fig. 4 [4]), and the tritiation is far from the piperidine ring. Whether this will increase stability is uncertain; however, the location will increase the yield of nitroxide (Fig. 4 [8]), and decrease steric hindrance. Also, another solvent will be used in the solution form during HPLC measurements. It is possible that during the drying procedure, tritium outgassing occurred because of the high boiling point of toluene at approximately 120 °C.

Our goal is to tritiate the compound first, and then apply it on a substrate (semiconductor device). Techniques will be developed to apply "cold" (untritiated) nitroxide on substrates representing semiconductor. The substrates would be planar and textured surfaces. After nitroxide synthesis, the compound will be dried down

to either gel or powder where its mass would be weighed in a known volume to calculate mass density. After mass density is measured, we will start investigating different coating procedures such as spin coating or sedimentation. The suitable coating technique will be used on the tritiated nitroxide with a planar and textured semiconductor device. A current and voltage (*I-V*) curve will be measured from the device for betavoltaic cell demonstration.

6. References

1. Thomas C, Portnoff S, Spencer MG. High efficiency 4H-SiC betavoltaic power sources using tritium radioisotopes. Applied Physics Letters. 2016;108:031505.

2. Li MG, Zhang J. A betavoltaic microcell based on semiconducting single-walled carbon nanotubes arrays/Si heterojunctions. Proceedings of the 2015 28th IEEE International Conference on Micro Electro Mechanical Systems (MEMS); 2015 Jan 18–22; Estoril, Portugal. Piscataway (NJ): IEEE; c2015. p. 1102–1105.

3. Tin S, Lal A. A radioisotope-powered surface acoustic wave transponder. Journal of Micromechanics and Microengineering. 2009;19(9): 094014.

4. Sychov M, Kavetsky A, Yakubova G, Walter G, Yousaf S, Lin Q, Chan D, Socarras H, Bower K. Alpha indirect conversion radioisotope power source. Applied Radiation and Isotopes. 2008;66(2):173–177.

5. Xu Z-H, Tang X-B, Hong L, Liu Y-P, Chen D. Structural effects of ZnS:Cu phosphor layers on beta radioluminescence nuclear battery. Journal of Radioanalytical and Nuclear Chemistry. 2014;303:2313–2320.

6. Russo J, Litz MS, Katsis D. Commercial-off-the-shelf (COTS) indirect energy conversion (IDEC) isotope design structure and power management. Adelphi (MD): Army Research Laboratory (US); 2014 Dec. Report No.: ARL-TR-7158.

7. Bower KE, Barbanel' YA, Shreter Y.G. Polymers, phosphors, and voltaics for radioisotope microbatteries. Boca Raton (USA): CRC Press; 2002.

8. Liu B, Chen KP, Kherani NP, Zukotynski S, Antoniazzi AB. Betavoltaics using scandium tritide and contact potential difference. Applied Physics Letters. 2008;92:083511.

9. Adams T, Revankar S. Research, development, and evaluation capabilities for betavoltaic power sources. Proceedings of the 122nd ASEE Annual Conference and Exposition; 2015 June 14–17; Seattle. WA. Paper ID #13983.

10. Kavetsky AG, Nekhoroshkov SN, Meleshkov SP, Kaminski YL, Akulov GP . Radioactive materials, ionizing radiation sources, and radioluminescent light sources for nuclear batteries. In: Bower KE, Barbanel' YA, Shreter YG, Bohnert GW, editors. Polymers, phosphors, and voltaics for radioisotope microbatteries. Boca Raton (FL): CRC Press LLC; 2002. p. 26–40.

11. Tozzini V, Pellegrini V. Prospects for hydrogen storage in graphene. Physical Chemistry Chemical Physics. 2012;15(1):80–89.

12. Zhou C, Chen S, Lou J, Wang J, Yang Q, Liu C, Huang D, Zhu T. Graphene's cousin: the present and future of graphane. Nanoscale Research Letters. 2014;9(1):26.

13. Zhu S, Li T. Hydrogenation-assisted graphene origami and its application in programmable molecular mass uptake, storage, and release. ACS Nano. 2014;8(3):2864–2872.

14. Xia Y, Yang Z, Zhu Y. Porous carbon-based materials for hydrogen storage: advancement and challenges. Journal of Materials Chemistry A. 2013;1:9365–9381.

15. Belovodskii LF, Gaevoi VK, Grishmanovskii VI. Tritium. Moscow: Energoatomizdat; 1985.

16. Nechaev YS. The high-density hydrogen carrier intercalation in graphane-like nanostructures, relevance to its on-board storage in fuel-cell-powered vehicles. The Open Fuel Cells Journal. 2011;4(1):16–29.

17. Sofo JO, Chaudhari AS, Barber DG. Graphane: A two-dimensional hydrocarbon. Physical Review B. 2007;75: 153401.

18. National Institute of Standards and Technology, Physical Measurement Laboratory. Estar: stopping-power and range tables for electrons. Washington (DC): National Institute of Standards and Technology; nd [accessed 2016 July 21] https://physics.nist.gov/PhysRefData/Star/Text/ESTAR.html.

19. Burks SR, Bakhshai J, Makowsky MA, Muralidharan S, Tsai P, Rosen GM, Kao JPY. 2H,15N-substituted nitroxides as sensitive probes for electron paramagnetic resonance imaging. Journal of Organic Chemistry. 2010;75(19):6463–6467.

20. Rosen GM. Use of Sodium cyanoborohydride in the preparation of biologically active nitroxides. Journal of Medicinal Chemistry. 1974;17(3):358–360.

21. Rosen GM, Schneider E, Shortkroff S, Tsai P, Winalski CS. Use of sodium triacetoxyborohydride in the synthesis of nitroxide biradicals. Journal of Chemistry Society. 2002;1:2663–2667.

22. Rosen GM, Rauckman EJ, Hord WW. Spin-labeled TMA analogs as probes to study the anionic site of acetylcholinesterase. General Pharmacology: The Vascular System. 1977;8(5–6):355–357.

23. Eriksson UG, Tozer TN, Sosnovsky G, Lukszo J, Brasch RC. Human erythrocyte membrane permeability and nitroxyl spin-label reduction. Journal of Pharmaceutical Sciences. 1986;75(4):334–337.

24. ViTrax Radiochemicals. Placentia (CA): ViTrax, Inc; c2013 [accessed 2016 June 6]. http://www.vitrax.com/.

25. Renschler CL, Clough RL, Shepodd TJ. Demonstration of completely organic, optically clear radioluminescent light. Journal of Applied Physics. 1989;66(9):4542–4544.

INTENTIONALLY LEFT BLANK.

Appendix A. Beta Source Parameter Calculations

Table A-1 Beta source variable symbols and definitions

Variable symbol	Variable definition
A_m	Specific activity, radioactivity per mass [Ci/g]
λ	Isotope decay constant [1/s]
N_A	Avogadro's constant
N	Total no. of atoms of the given elements in the molecule
χ	Ratio of radioactive atoms to total no. of atoms of the given element
M_m	Molecular mass in grams of the carrier substance comprising the element incorporating the radioactive isotope of interest.
P_{sp}	Specific power per 1 Ci, the minimal significant activity of the isotope [μW_n/Ci]
ε_β	Beta energy [eV]
ε_{avg}	Mean beta energy [eV]
ε_{max}	Maximum beta energy [in units of MeV]
μ_m	Mass absorption coefficient of betas [cm^2/g]
$D_{0.99}/D_L$	Layer thickness, the tritium-containing substance layer thickness $D_{0.99}$ – saturation thickness D_L – ESTAR thickness following Thomas et al.[1]
dP_β/dS	Specific beta flux power/power density [$\mu W_n/cm^2$]
GD	Gravimetric density, percentage of radioactive atoms' atomic mass over a total molecular mass
VD/ρ_T	Effective density of the tritium inside the carrier system
V_{As}	Volume radioactivity, radioactivity per unit volume
S_m	Effective surface activity, radioactivity per surface area [mCi/cm^2]

$$A_m = \frac{\lambda N_A N \chi}{3.7\times10^{10}\, M_m} \tag{A-1}$$

$$P_{sp} = 3.7 \times 10^{10} \int_0^1 w(\varepsilon_\beta)\varepsilon_\beta d\varepsilon_\beta = 3.7 \times 10^{10}\ \varepsilon_{av} \tag{A-2}$$

$$\mu_m = 15.5\varepsilon_{max}^{-1.41} \tag{A-3}$$

$$\frac{dP_\beta}{dS} = \frac{A_m P_{sp}}{2(\mu_m)} \int_0^1 z[1 - \exp((\mu_m\, D_L)/z)]dz \tag{A-4}$$

$$S_m = \frac{\frac{dP_\beta}{dS}}{3.7\times10^{7} * \varepsilon_{avg} * (1.6\times10^{-16})} \tag{A-5}$$

Equations are based on the point beta source dose function for thin-layer sources. Bower et al.[2] calculates dP_β/dS by multiplying specific activity (A_m) with 9×10^4 μW_n*g/(Ci*cm^2). This factor accounts for the efficiency of conversion of beta-particle energy in the decay into the energy of the beta flux let out from the

[1] Thomas C, Portnoff S, Spencer MG. High efficiency 4H-SiC betavoltaic power sources using tritium radioisotopes. Appl Physics Lett. 2016;108:031505.

[2] Bower KE, Barbanel YA, Shreter Y.G. Polymers, phosphors, and voltaics for radioisotope microbatteries. Boca Raton (USA): CRC Press; 2002.

beta source containing carrier substance to its surface. P_{sp} and μ_m are included in this factor shown in Eq. A-4. There is less than a 7% difference between the calculated and experimental dP_β/dS and S_m of scandium tritide (Sc^3H_2) and titanium tritide/tritiated titanium hydride (Ti^3H_2) foils. Differences in theoretical and experimental values could be due to certain assumptions such as complete tritiation of foils and homogenous concentration of tritium in foil. However, the error between theoretical and experimental values cannot be identified for the other tritiated compound due to lack of empirical results. There most likely will be error since these equations were formulated by the experimental results of metal foils.

INTENTIONALLY LEFT BLANK.

Appendix B. Total Specific Activity Calculations of MCNPX Model

B-1 ^{3}H-nitroxide Calculations

The simulated tritium (^{3}H)-nitroxide compound has M_w = 176 g/mol with 3 tritium atoms. If the mass density is 0.1 g/cm^3 in a 10-μm layer, then there is 10^{-4} g of tritium. The volume of the thin layer is

$$v = 10\,\mu m \times 1\,cm^2 = 0.001\,cm^3. \quad \text{(B-1)}$$

Number of moles in volume

$$1 \times 10^{-4} g \times \frac{1\,mol}{176\,g} = 5.68 \times 10^{-7} mol. \quad \text{(B-2)}$$

Number of tritium atoms in volume

$$3\ {}^3H \times 5.68 \times 10^{-7} mol \times 6.023 \times 10^{23} \frac{atoms}{mol} = 1.03 \times 10^{18} atoms\ of\ {}^3H\,. \quad \text{(B-3)}$$

Number of curies in volume

$$1.705 \times 10^{-6} mol\ of\ tritium \times 3 \frac{g}{mol} \times 9700 \frac{Ci}{g}^{1} = 49.6\,mCi. \quad \text{(B-4)}$$

S_m of a single layer side with an area of 1 cm^2 (~11.5% leaving a thin layer surface)

$$S_m \approx 5.7\ \frac{mCi}{cm^2}. \quad \text{(B-5)}$$

Including both sides of thin layer (~23%)

$$S_m \approx 11.4\ \frac{mCi}{cm^2}. \quad \text{(B-6)}$$

Our near-term goal is S_m = 30 mCi/cm^2 from a single side of the layer. The theoretical calculations and MCNPX model show that the tritiated compound is far from reaching our near-term goal. Tritium content would need to be 5 times the tritium atoms with the same molecular weight to reach our goal. Compound 4, Scheme 4 (Fig. 5 [2, 3] in main report), can reach close to 30 mCi/cm^2 for a single side. The compound has already been fully deuterated. The major setback is the unknown stability of the tritiated compound. It is quite possible that the compound degrades completely during tritiation because of such a high tritium concentration

[1] Appendix A to Part 71—Determination of A1 and A2. NRC: 10 CFR 71, Appendix A—Determination of A1 and A2. N.p., n.d. Web. 01 Aug. 2016. http://www.nrc.gov/reading-rm/doc-collections/cfr/part071/part071-appa.html.

of 26 wt% ^{3}H. Further studies and experimental testing with deuterium must be performed before deciding on performing Scheme 4.

B-2 Ti^3H_2 Calculations

The simulated titanium tritide/tritiated titanium hydride (Ti^3H_2) metal foil has M_w = 54.0 g/mol with 2 tritium atoms. If the mass density is 3.91 g/cm^3 in a 400-nm layer, then there is $4.00 \times 10^{-5} cc$ volume. The volume of the thin layer is

$$v = \ 400\ nm \times 1\ cm^2 = \ \ 4.00 \times 10^{-5}\ cm^3. \qquad \text{(B-7)}$$

Number of moles in volume

$$4.00 \times 10^{-5}\ cm^3 \times 3.91 \frac{g}{cm^3} \times \frac{1\ mol}{54\ g} = 2.90 \times 10^{-6}\ mol. \qquad \text{(B-8)}$$

Number of tritium atoms in volume

$$2\ {}^3H \times 2.90 \times 10^{-6}\ mol \times 6.023 \times 10^{23} \frac{atoms}{mol} = 3.49 \times 10^{18} atoms\ of\ {}^3H\ . \text{(B-9)}$$

Number of curies in volume

$$5.80 \times 10^{-6}\ mol\ of\ tritium \times 3 \frac{g}{mol} \times 9700 \frac{Ci}{g}\ ^1 = 169\ mCi. \qquad \text{(B-10)}$$

S_m of a single layer side with an area of 1 cm^2 (~23% leaving a thin layer surface and 80% loaded)

$$S_m \approx 31.1\ \frac{mCi}{cm^2}. \qquad \text{(B-11)}$$

Including both sides of thin layer (~23%)

$$S_m \approx 62.2\ \frac{mCi}{cm^2}. \qquad \text{(B-12)}$$

Figure B-1 shows a plot of the energy percentage leaving the layer and penetrating GaN surfaces.

[1] Appendix A to Part 71—Determination of A1 and A2. NRC: 10 CFR 71, Appendix A—Determination of A1 and A2. N.p., n.d. Web. 01 Aug. 2016. http://www.nrc.gov/reading-rm/doc-collections/cfr/part071/part071-appa.html.

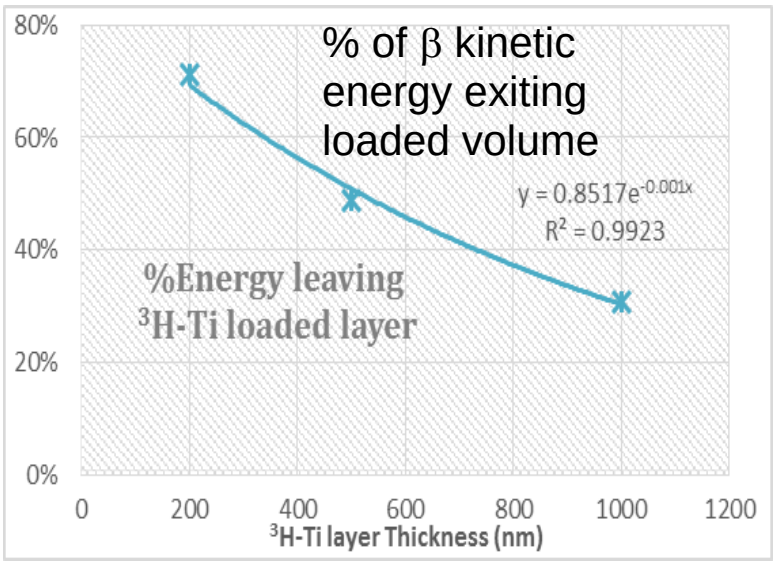

Fig. B-1 Percentage of beta kinetic energy exiting the loaded volume as function of layer thickness

Appendix C. High-Performance Liquid Chromatography (HPLC) Brief Description

A high-performance liquid chromatograph (HPLC) is used to separate, identify, and quantify tritiated compounds. A typical HPLC consists of a sampler, pump, column, and detector. The precursor is analyzed by HPLC to measure the purity of the sample before tritiation. All samples are dissolved in HPLC-grade toluene. The solvent is required to create a mobile phase. The mobile phase transports the sample through the HPLC system. The pump delivers the desired flow and composition of the mobile phase through a column. The column is a tube filled with solid adsorbent material such packing materials (pellicular or porous particles). The mobile phase shifts to a stationary phase after entering the column. The sample, possibly made up of various types of compounds, is separated based on different degrees of interaction with the particles due to polarity. Typically, a UV-visible detector is the detection method. For UV light, the amount of light absorbed will depend on the amount of a particular compound that is passing through the beam at the time. The output of the received signal will be recorded as retention time peaks displayed in a chromatogram. Retention time length is directly related to molecule polarity. For example, silica particles are polar inside the column. The polar molecules bind/adsorb to it while the nonpolar molecules will pass more quickly through the stationary phase. For radioactivity detection, a radio flow detector system is used. Low noise photomultipliers operating with an optimized coincidence circuitry and luminescence subtraction with liquid scintillation provide the best sensitivity available to detect radioactivity of sample.

List of Symbols, Abbreviations, and Acronyms

1-D	1-dimensional
2-D	2-dimensional
3-D	3-dimensional
A_m	specific activity
ARL	US Army Research Laboratory
COTS	commercial-off-the-shelf
$D_{0.99}$	saturation thickness layer
D_L	optimal thickness layer
dP_β/dS	specific beta flux power, also called power density
EHPs	electron-hole pairs
FOM_{2D}	figure of merit of 2-D betavoltaic configuration
FOM_{3D}	figure of merit of 3-D betavoltaic configuration
GD	gravimetric density
GaN	gallium nitride
HAGO	hydrogenation-assisted graphene origami
HPLC	high-performance liquid chromatography
^{63}Ni	nickel-63
NO_x	nitroxide for tritiation
OED LLC	Organic Electronic Devices LLC
PDA	photodiode array
^{3}H	tritium
$Sc^{3}H$	scandium tritide
TEMPO	4-methoxycarbonyl-methylene-2,2,6,6-tetramethyl-1-piperidinyloxyl
$Ti^{3}H_x$	titanium tritide/tritiated titanium hydride
S_m	effective surface activity

STP	standard temperature and pressure
UV	ultraviolet
vDw	van der Waals
V_m	volume activity (Ci/cm^3)

1 (PDF) DEFENSE TECHNICAL INFORMATION CTR DTIC OCA

2 (PDF) DIRECTOR US ARMY RESEARCH LAB RDRL CIO L IMAL HRA MAIL & RECORDS MGMT

1 (PDF) GOVT PRINTG OFC A MALHOTRA

3 (PDF) DIRECTOR US ARMY RESEARCH LAB RDRL SED E J A RUSSO W B RAY II M S LITZ

INTENTIONALLY LEFT BLANK.